J Paleolimnol (2020) 63:65–81
https://doi.org/10.1007/s10933-019-00103-2

ORIGINAL PAPER

pH-dependent silicon release from phytoliths of Norway spruce (*Picea abies*)

Zsuzsa Lisztes-Szabó · Anna F. Filep · Attila Csík · Ákos Pető · Titanilla G. Kertész · Mihály Braun

Received: 15 May 2019 / Accepted: 14 November 2019 / Published online: 26 November 2019

Abstract Accurate evaluation of the preservation state of fossil phytoliths in glacial lake sediments is important, as these microfossils are often used in paleoecological and archaeological studies. The characteristic phytolith type of the Norway spruce (*Picea abies* [L.] Karst.) needle is a potential keystone in paleoecological studies. In this laboratory study, we investigated dissolution of *Picea abies* blocky type phytoliths, to simulate dissolution processes in sediments and soils and create reference material to compare with fossil phytoliths. Intact needles, needle ash, diatomite and silica gel were treated with Britton–Robinson buffer solutions at pH values from 2 to 12 for 22 days. Silicon was measured by microwave plasma atomic emission spectrometry. Treatment effects were evaluated on longitudinal cuts of needles under a stereomicroscope and on phytolith assemblages from needles using a light microscope. Surfaces of treated phytoliths were investigated by scanning electron microscope and elemental analysis of phytoliths was determined by energy dispersive X-ray fluorescence. Dissolution of silicon in spruce needles was inhibited between pH 8.0 and 11.1. Needle tissue protects phytoliths from erosion processes at this alkaline pH range. Most dissolved silicon appeared to originate from the phytolith surfaces and the silica matrix of the apoplast in the tissues, with less from complete dissolution of phytoliths. Our experiment suggests that extraneous metal elements are incorporated into the silica structure during the dissolution process. Thus, higher element content is an effect of partial dissolution rather than a cause of dissolution. Ultrastructure of the surface of *Picea*-blocky type

Electronic supplementary material The online version of this article (https://doi.org/10.1007/s10933-019-00103-2) contains supplementary material, which is available to authorized users.

Z. Lisztes-Szabó (✉) · A. F. Filep · T. G. Kertész · M. Braun
Isotope Climatology and Environmental Research Centre, Institute for Nuclear Research, Hungarian Academy of Sciences, Debrecen, Hungary
e-mail: lisztes-szabo.zsuzsanna@atomki.mta.hu

A. F. Filep
e-mail: filepanna@atomki.mta.hu

T. G. Kertész
e-mail: titanilla.kertesz@atomki.mta.hu

M. Braun
e-mail: mbraun@atomki.mta.hu

A. Csík
Institute for Nuclear Research, Hungarian Academy of Sciences, Debrecen, Hungary
e-mail: csik.attila@atomki.mta.hu

Á. Pető
Institute of Nature Conservation and Landscape Management, Szent István University, Gödöllő, Hungary
e-mail: peetoako@gmail.com

phytoliths, namely disappearance of the globular structure, may be useful to assess the intensity of destructive processes in sediments. Our experimental treatments indicate that characteristic *Picea*-blocky phytoliths in needles can be well-preserved, depending on circumstances in sediments. Further micro-analytical measurements will make these needles promising tools for paleoenvironmental reconstructions.

Keywords Dissolution · Elemental composition · Reference study · SEM · Surface structure · Taphonomy

Introduction

Silica bodies or phytoliths ($SiO_2 \cdot nH_2O$) are created in many plant species as a consequence of monosilicic acid uptake. These structures are analyzed in paleoecological and archaeological studies because of their taxonomic relevance and persistence in soils and sediments after the plant degrades (Hart 2016). A characteristic phytolith type was recently recognized in the transfusion tissue of Norway spruce (*Picea abies* [L.] Karst.) needles (Lisztes-Szabó et al. 2019). This may be a potential keystone in future paleoecological studies for several reasons: (1) Norway spruce was an important species in the northern hemisphere during the early Holocene (Latałowa and van der Knaap 2006; Magyari et al. 2014; Molnár and Végvári 2017); (2) spruce needles are often present and well preserved in sediment cores of glacial lakes and peat bogs; (3) phytoliths may be obtained from fossil needles, making it unnecessary to separate discrete phytoliths from the sediment by difficult and time-consuming microfossil preparation protocols; (4) needle fossils preserve phytoliths in the tissues in situ, and can be further investigated with micro-chemical techniques (SEM–EDX, LA-ICP-MS); and (5) this special blocky form (*Picea*-blocky type), which develops in the needle, is a characteristic and recognizable silica body in phytolith assemblages from sediments.

Presence or absence of this phytolith type in fossil spruce needles may depend on environmental conditions (Lisztes-Szabó et al., unpublished results). Using this feature of needles to better understand paleoecological processes may make it possible for us to determine the circumstances of their development and preservation. To use these phytoliths as a proxy for terrestrial climate, we have to clarify how sensitive they are to different environmental conditions.

Accurate evaluation of the preservation state of fossil phytolith assemblages is important for paleoecological reconstructions. Preservation of phytoliths varies across species and morphotypes, making it necessary to study their taphonomy before they can be used in paleoecological reconstructions (Shillito 2011; Madella and Lancelotti 2012; Cabanes and Shahack-Gross 2015). Preservation of the phytoliths of a species and their morphotypes in sediments depends on many factors, including weathering processes and sediment pH (Wilding and Drees 1974; Piperno 2006). The surface of phytoliths has considerable relevance from the aspect of dissolution kinetics, but according to Fraysse et al. (2009), this may not be the most important factor. Stability is not the same for all phytolith morphotypes. According to Bartoli and Wilding (1980), and Nguyen et al. (2014), phytoliths of different anatomical origins may contain different elements, which may affect their stability. In contrast, Fraysse et al. (2009) found no correlation between Al content and the solubility of phytoliths. Thus, it is unclear whether Al stabilizes phytoliths or not. Without doubt, solubility of silica bodies depends on the stage of phytolith development, namely their maturity (Osterrieth et al. 2009). The importance of understanding the elemental composition of phytoliths and concentration changes of minor constituents such as aluminum, carbon and other elements, was emphasized by Alexandre et al. (2015, 2016).

Silica in plants is an important component of the silicon geochemical cycle because it is more available than silicon originating from minerals (Derry et al. 2005; Fraysse et al. 2009; Puppe et al. 2017). The influence of phytolith biogenic silica content on ecosystems was shown by several authors (Wang et al. 2011; Ran et al. 2018). Moreover, about 90% of silicon accumulated by plants is in phytoliths (Song et al. 2014). There is increasing interest in the impact of phytoliths on the Si cycle, especially with respect to land management, i.e. forest or cropland.

Most phytolith-dissolution experiments were done on prepared phytoliths, with a focus on investigation of their dissolution kinetics. Few studies have reported

on the dissolution behavior of phytoliths in plant tissues. Puppe et al. (2017), however, reported that a silicon pool evolves through release of silicon in soils, because phytogenic Si in plant tissues is temporarily protected from dissolution. Studying dissolution of phytoliths in tissues may enable more accurate estimates of the amount of dissolved silicon from fossil and subfossil needles, and provide a better understanding of phytolith taphonomy.

We studied the pH-dependent dissolution and alteration of phytoliths in the tissue of spruce needles (in situ). Our aim was to create a reference treatment using a buffer series, which covered a broad pH range that occurs in nature. Taphonomic aspects of pH-dependent morphological changes of phytoliths were considered, along with shifts in elemental content. Stability and dissolution features of *Picea*-blocky type phytoliths were revealed. The pH-dependent dissolution of silica in spruce needles was compared with the responses of amorphous inorganic and biogenic silicates under the same conditions. Taphonomic and biochemical aspects of spruce phytoliths were also considered.

Materials and methods

Dissolution experiments were conducted on diatomite, silica gel, spruce needles, and needle ash in buffer solutions at different pH. According to our aims, we were focusing on the parameters of phytoliths in tissue-condition. Thus, the treated spruce needles were used in further investigations (phytolith analysis under stereo-, light and scanning electron microscope, element analysis).

Pretreatment of spruce needles

Silica accumulates in spruce leaves continuously over time (Hodson and Sangster 1998). We collected three-year-old or older needles from a reference tree, which was growing in a private yard in the Great Hungarian Plain (47.553296° N, 21.599187° E). This tree was selected because it was the subject of earlier studies (Lisztes-Szabó et al. 2019).

Wet weight of the collected needles was 163 g. They were placed into a 1000-mL polypropylene vessel and 750 mL of ultrapure water (Arium Pro, Sartorius, resistivity > 18.2 M Ω cm^{-1}) was added to the sample. Ultrapure water was used to wash and prepare all solutions during this study.

Vessels containing needles were placed in a shaker (KS-15, Edmund Bühler GmbH) for 30 min, and subsequently in an ultrasonic bath (Elmasonic, S180H) for 10 min. Needles were filtered with a plastic sieve. Washing was repeated twice. Needles were then dried at 105 °C overnight. Wax from the surface of needles was removed by washing with 500 mL of chloroform (analytical grade, Molarchem). Needles were dried again at 105 °C. Dry weight of the remaining sample was 83.5 g, and these leaves were used for all experiments.

Ashing of needles

Ashing of needles was required to prepare phytoliths for microscopic investigation and for producing ash to carry out dissolution studies. A muffle furnace (Nabertherm N641) was used and the temperature was increased by a rate of 100 °C h^{-1} to 500 °C. This temperature was held for 3 h. Needles were ashed in porcelain crucibles that had been stored in 1:5 nitric acid for at least 24 h. After rinsing with ultrapure water, the crucibles were dried at 105 °C and then heated at 500 °C for 2 h. Pretreated crucibles were stored in sealed plastic bags.

Diatomite and silica gel

Diatomite is a biogenic silicate that is widely used in silicon studies (Alexandre et al. 1997; Ran et al. 2018). We used diatomite collected from a former kaolinite mine (Borovany, Czech Republic, 48.916263° N, 14.637597° E, provided by K. Buczkó, pers. commun.). Silica gel (63–200 µm, Molar Chemicals, ref. no.: R55161817) was used as an abiotic non-crystalline silicate.

Buffer solutions

Britton–Robinson buffer solutions were used in the dissolution experiment (Britton and Robinson 1931; Mongay and Cerda 1974). The Britton–Robinson buffers consist of acidic (CH_3COOH, H_3PO_4, H_3BO_3) and alkaline (NaOH) components, and display a range of pH from 2 to 12. The exact pH value is set by the amount of alkali in solution (Britton and Robinson 1931; Mongay and Cerda 1974). We

compounded 16 buffers to obtain the full pH range covered by this type of buffer. Solutions were freshly prepared and their pH values were measured with an HQ40D Portable Multi Meter. The pH was also recorded at the end of the experiments. No significant change in pH was observed in any of the cases.

Dissolution experiments and measurement of silicon

For spruce needle (treated needle–TN), diatomite and silica gel samples, 0.50 g of material was placed into 50-ml centrifuge tubes containing 45 ml of the Britton–Robinson buffer solution. Polypropylene centrifuge tubes with a volume of 50 mL were used for the dissolution studies. Tubes were not filled completely, to enable efficient shaking.

In the case of the spruce needle ash experiment (treated ash–TA), 0.50 g of needles were measured into crucibles. Needles were ashed as described above, and the ash was transferred into the centrifuge tubes. In this way, the silicon content of plant material was kept constant.

The plastic tubes that contained samples were then placed in a shaker (Edmund Bühler GmbH, KS-15). Every other day during the first 10 days, and then every fourth day, shaking was stopped, tubes were centrifuged, and a sub-sample was taken to determine the silicon content. The volume of each subsample removed was 0.50 mL, and was collected from the supernatant and transferred into a 15-mL centrifuge tube. Volume was brought to 10 mL with ultrapure water.

Although it has been suggested that one week is sufficient to reach equilibrium with respect to dissolution of phytoliths (Cabanes and Shahack-Gross 2015), we continued the dissolution experiments for 22 days. The dissolution experiments using silica gel and diatomite were stopped on day 10, because there was no measurable increase in concentration of silicon by that time.

The measurement of silicon was carried out by microwave plasma atomic emission spectrometry (MP-AES), using an Agilent 4100 instrument. The atomic emission line of Si (251.611 nm) was used. Standards were prepared from 10,000 mg L^{-1} Si stock solution (CPAchem, Ref. no. C153.W.L1). The limit of quantification of the method was 50 µg L^{-1}.

Phytolith analysis

Longitudinal cuts of a few spruce needles were studied under a stereomicroscope (Zeiss Stereomicroscope Discovery v20) after treating them with a series of buffer solutions for 22 days. Photos were taken of material from each pH treatment.

Phytolith extraction from treated needles (TNs) was accomplished using the dry-ashing technique (Albert and Weiner 2001; Mercader et al. 2010; Lisztes-Szabó et al. 2019). Samples were dried at 105 °C overnight and weighed. Next, samples were combusted in a furnace at 500 °C for 8 h in air, then 3 mol L^{-1} HCl and 3 mol L^{-1} HNO_3 solution were added and the ash was treated for 30 min at 100 °C. The acid-insoluble fraction was centrifuged three times (3000 rpm for 2 min) and the supernatant was discarded. Next, hydrogen peroxide (30% H_2O_2) was added to the pellet, and samples were dried at 105 °C and weighed. The resulting mass was the biogenic silica content that is usually reported as the percent of sample dry weight. This sample hereafter is referred to as treated needle ash (TN ash) to distinguish from the treated ash (TA).

TN ashes were mixed thoroughly and phytoliths were mounted on microscope slides in immersion oil and observed under an Alpha Euromex CMEX-5 polarized light microscope at a magnification of 400x. Optically isotropic phytoliths were verified using cross-polarized illumination. In addition, the phytolith samples were deposited in Eppendorf tubes in the Phytolith Collection of the Isotope Climatology and Environmental Research Centre (ICER) with laboratory code 115-1525.1-16. Five hundred phytoliths per species were counted in adjacent, but not overlapping lines across the cover slip. Phytolith morphotypes were documented by microphotographs (ImageFocus, version 4). Large fragments of silicified tissues were considered to be representative features, but intercellular deposits or other small and undefined fragments were not included in the count. The number of tissue fragments, eroded, and non-eroded *Picea*-blocky phytoliths were counted, and other phytolith morphotypes were put into a common "other morphotypes" group.

Phytolith SEM–EDX microanalysis

Longitudinal cuts of TNs and some ashes from the TNs were spread with a paintbrush onto double-sided

tape mounted on an aluminum stub and the ash sample was coated with gold (Bio-Rad E5000C Sputter Coater). Four well-characterized *Picea*-blocky type phytolith forms were measured randomly for elemental analysis in the tissue and in the ash at four pH values (2, 9, 10, 12). These pH values were deemed important because of the Si dissolution curve from the spruce needle experiment. Elemental analysis of phytoliths was conducted using a Hitachi S4300-CFE scanning electron microscope with energy dispersive X-ray fluorescence, operating at 15 kV with a detection threshold of 0.1 atom%. Principal component analysis was undertaken (using PAST, Hammer et al. 2001) on correlation matrices after logarithmic transformation of the element data.

Results

Silicon content and solubility of phytoliths

The average silicon content of the spruce needles was 5.3 ± 0.5 g kg^{-1}. With an exponential increase above pH 11, dissolution curves of the silica gel and the diatomite were similar to the expected theoretical Si dissolution pattern (Fig. 1). The silicon content of the solution of silica gel did not show considerable change over time, increasing by only about 21 mg L^{-1} in the acidic solutions by day 10 (from 21.0 to 42 mg L^{-1}; pH 5.8). Also, the diatomite Si concentration changed little with time in alkaline solution, increasing by about 45 mg L^{-1} by day 10 (from 53.7 to 98.5 mg L^{-1}; pH 11.2). Silicon solubility in silica gel and diatomite was highest at pH 11.9 (approximately 217 mg L^{-1}), much more than the total amount of average Si in spruce needles (Fig. 2).

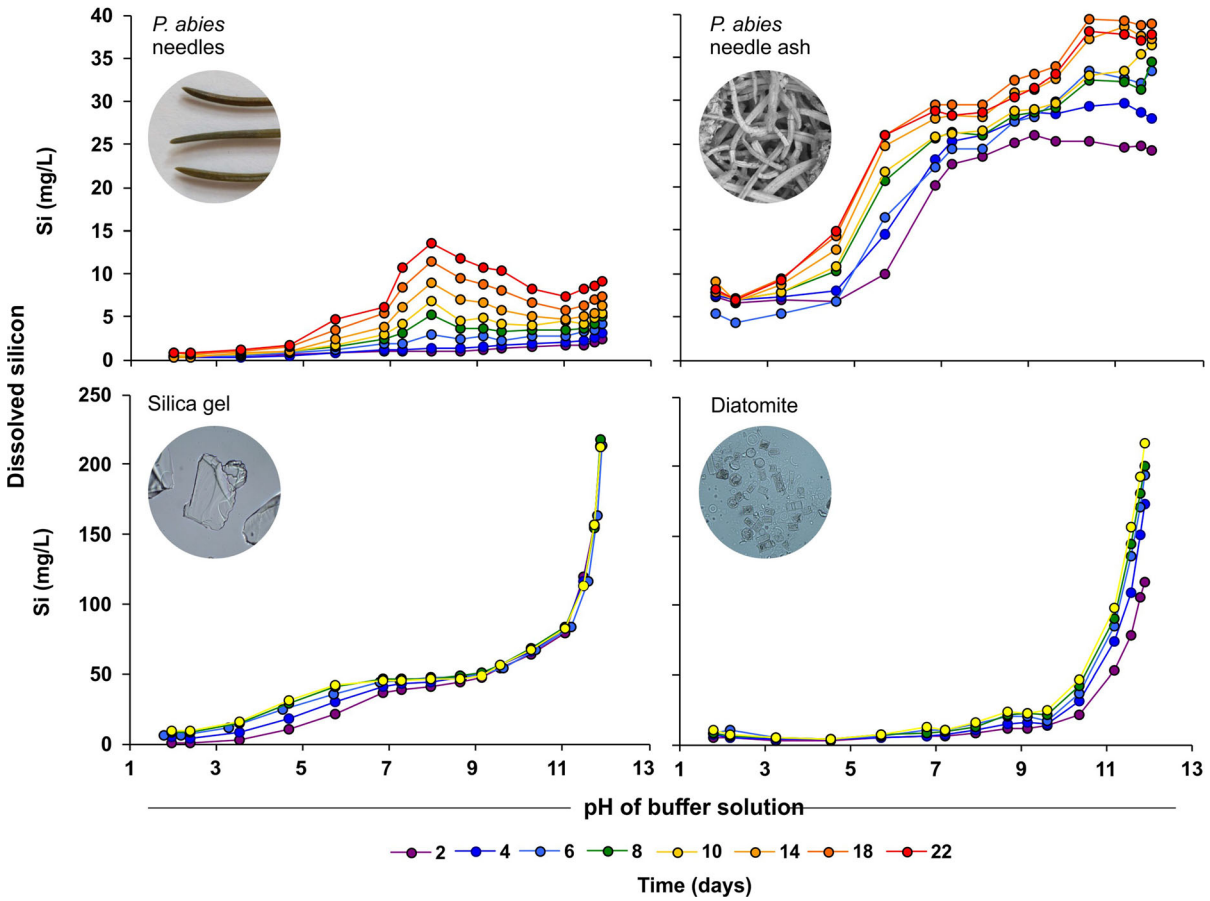

Fig. 1 Dissolved silicon content of the solution of spruce needles, ash of needles, silica gel and diatomite at pH 2–12. (Color figure online)

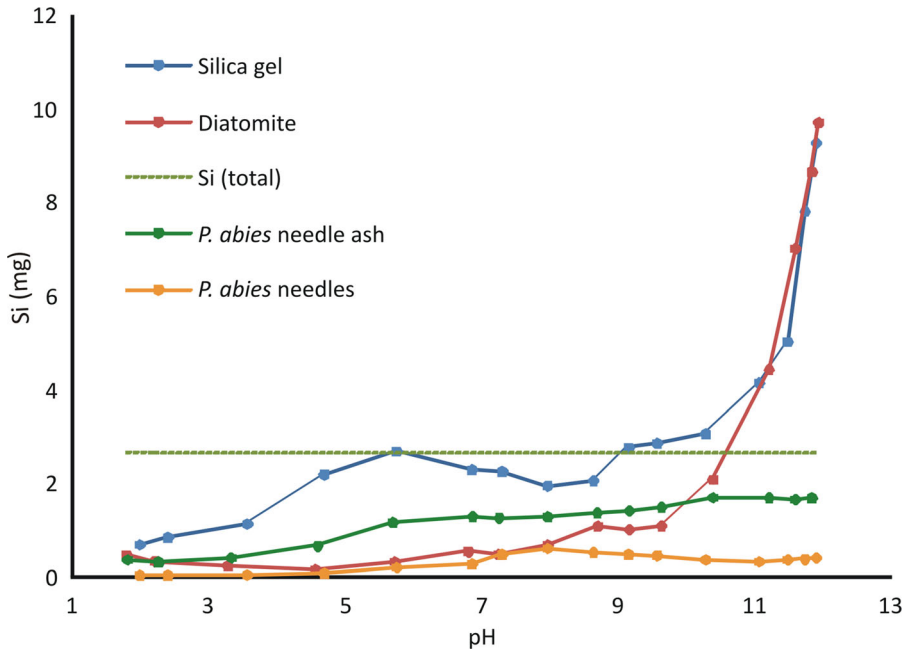

Fig. 2 Solubility of the silicon of spruce needles, ash of needles, silica gel and diatomite at different pH values on day 22. Dashed line (Si total) shows the total amount of average Si content in the spruce needles. (Color figure online)

Consequently, buffer solutions were able to dissolve the total amount of silicon content in the spruce needles.

In contrast, the amount of silicon dissolved from the spruce needles (TN) showed a specific dissolution curve (Fig. 1). At pH 3.6, this started to increase moderately with pH, but the intensity of dissolution decreased above pH 8.0. Above pH 11.1, dissolution increased again with greater pH. Between pH 3.6 and 11.9 the silicon content of the solution increased continuously with time, and did not stop on day 22. The dissolved silicon content of the solution was 13.6 mg L^{-1} at pH 8.0 on day 22, the highest value measured during the experiment.

The dissolution curve of spruce needle ash (TA) was different from that of the TNs themselves (Fig. 1). At pH 3.3, this began to increase moderately with pH, then the first high value of dissolution occurred at pH 7.3, 29.5 mg L^{-1} on day 18. After a small decrease at pH 8.0 (28.6 mg L^{-1} on day 18), dissolution again increased with pH. The silicon content of the solution did not increase by day 22, and the highest silicon content was 39.3 mg L^{-1} at pH 10.4 on day 18, almost three times greater than the highest value recorded for the dissolution of needles. In the case of both TNs and TAs, the total silicon content was not dissolved by day 22 of the experiment (Fig. 2).

Changes of morphotypes

After treatment at different pH values, phytoliths of TNs were studied in situ, i.e. in the needle tissue under a stereomicroscope (Fig. 3). There was no significant difference between the number of phytoliths in TNs at different pH values. Several phytoliths were seen at pH 2.0 and at pH 12.0 (Fig. 3). At pH 8.0, needles contained phytoliths, but a few needles presented without phytoliths (Fig. 2).

There were two different forms of dissolved phytoliths in the ash of the TNs. One was a dissolved type with cavities in the phytolith. This is a frequent dissolution indicator that occurs on the surfaces of elongate phytolith types and the guard cells of the stomata (Fig. 4a–c). The other abundant dissolution type was the darker, eroded type, which was often cracked or broken (Fig. 4e–f). As expected, the number of partially dissolved morphotypes and fragments increased with pH, but there were also unmodified phytoliths (Fig. 4d).

Changes in the *Picea*-blocky morphotype were studied and the amount of other phytolith

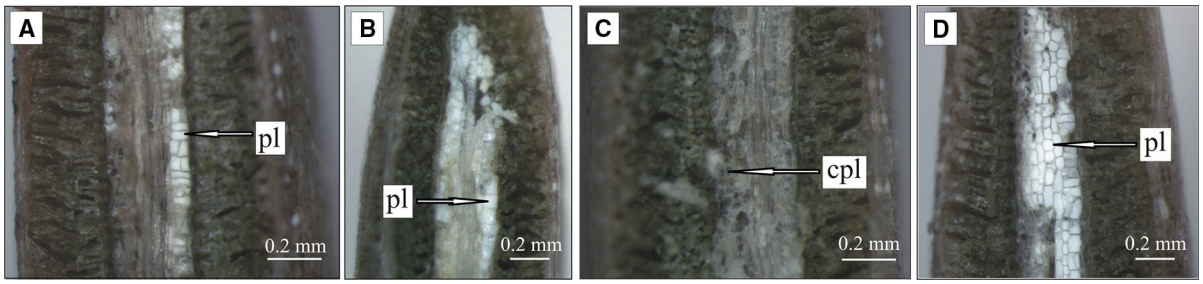

Fig. 3 Stereomicroscopic pictures of the longitudinally cut spruce needles after treatment at different pH values. **a** pH 2.0, **b** pH 8.0, **c** pH 8.0, **d** pH 11.9. *pl* phytoliths, *cpl* cavity of phytolith (encapsuled by cellwalls)

morphotypes and the silicified tissues were counted (Fig. 5). Percentages of the dark, eroded, blocky phytolith morphotype increased with pH in acidic buffers, and the highest value (51%) was found at pH 6.9. At alkaline pH, numbers of eroded phytoliths were smaller. On the other hand, the number of uneroded phytoliths decreased continuously with the increasing pH. At pH values for which Si dissolution was considerable, the percent of silicified tissues decreased, whereas the number of other morphotypes increased.

Phytolith surface changes evaluated by SEM

To understand phytolith changes associated with dissolution and to acquire comparative data on eroded phytoliths, we studied their surfaces by SEM. The phytolith surfaces of the TNs were compared to untreated, control material. Untreated blocky-type phytoliths have a specific ultrastructure with tiny granules of opal (Fig. 6a, b), and we also found this characteristic structure on the surface of TN phytoliths at pH 2.0 (Fig. 6c, d). This ultrastructure is typical for phytoliths treated at acidic pH, whether in the TN ash (Fig. 6c) or in situ, in the TN tissue (Fig. 6d). As the light-microscopic pictures show, there were unambiguous signs of dissolution on the phytolith surfaces in alkaline solutions, as these surfaces became dark. After treating the needles at pH 9.1 and 10.4, the phytoliths became smoother, as tiny particles fused into a more or less flat surface seen under the SEM (Fig. 6e, f). This surface structure was typical of phytoliths that originated from TN tissue and TN ash. Phytoliths from the TN ash show pitted surfaces at pH 9.1 (Fig. 6f).

At pH 11.9, we found eroded phytoliths, similar to surfaces described above in the ash and tissues (Fig. 7a–d). Broken and eroded phytoliths, with dissolved cavities, were also found (Fig. 7d–f).

Element concentrations

Several dark-colored phytoliths were found in TNs at alkaline pH. One of our aims was to establish the reason for this, using EDX measurements on phytoliths in TN tissues and in the TN ash. Differences in element contents between phytoliths treated at acidic and alkaline pH are clear (Fig. 8). At acidic pH, EDX revealed only carbon, silicon and oxygen in phytoliths in ash and tissue. In control phytoliths, and phytoliths treated with alkaline pH, however, aluminum, magnesium, calcium, and potassium were found in various amounts in ashed and tissue phytoliths (Fig. 8). Control phytoliths did not contain sodium in measurable amounts, in contrast to phytoliths treated at alkaline pH. Compared with the reference data from untreated phytoliths, our results showed that the diversity of elements in phytoliths was lower at acidic pH. There were no significant differences in element content between phytoliths from ashes and tissues, or among the different pH treatments.

PCA showed that the first three principal components account for 60%, 28%, and 10% of the variability in the data, with the first two principal components accounting for 88%. Additional principal components did not add considerable information. Two or three groups can be distinguished. First, the pH 2–12 group, second is the pH 9–10 group, and the third may be the reference group, but its separation from the pH 2–pH 12 groups is only clear a priori (Fig. 9). The results show that the element concentrations in the ash

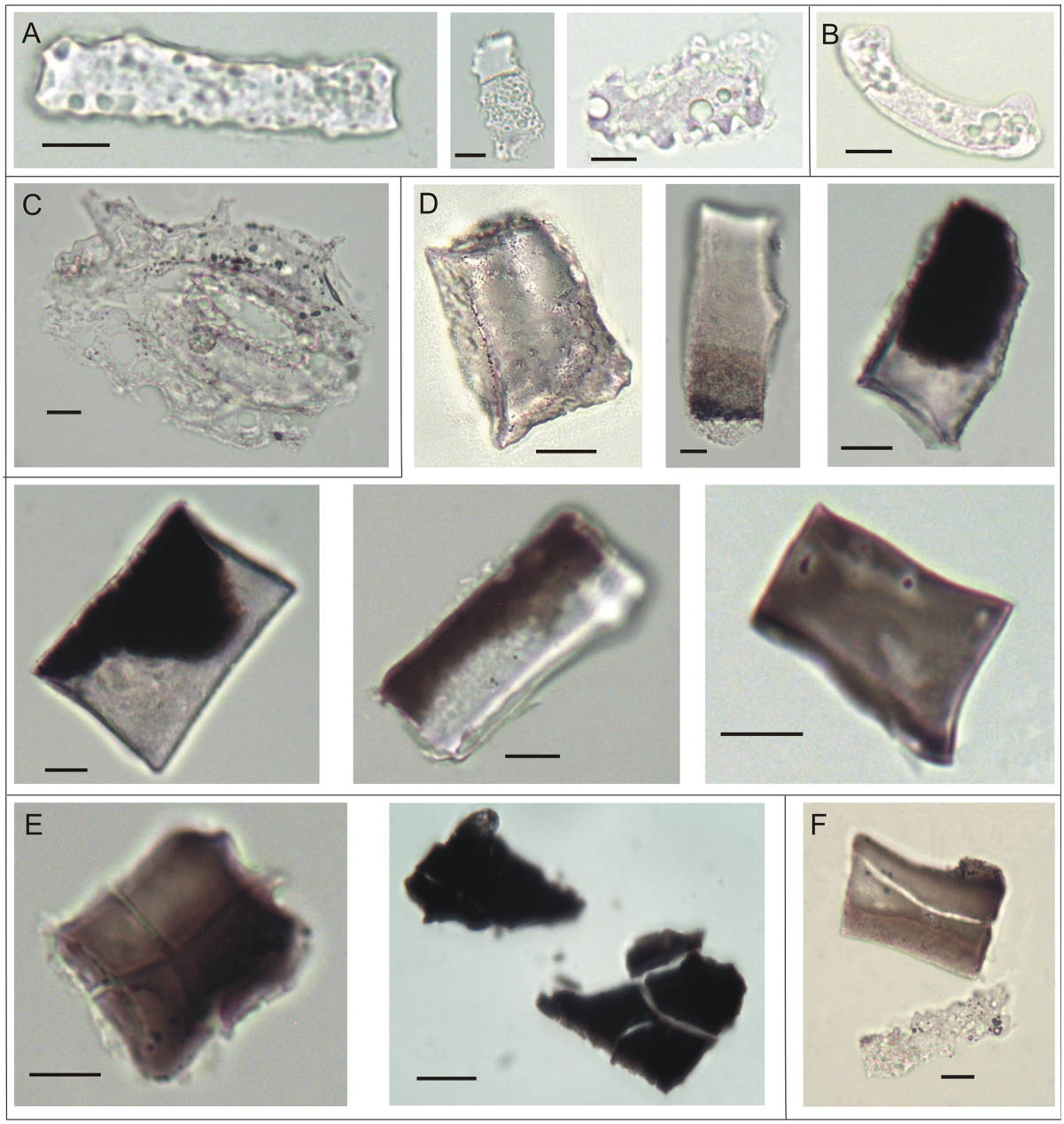

Fig. 4 Partially dissolved spruce phytoliths from the ash of the needles (TNs) treated at different pH solutions. **a** elongate epidermal phytoliths with dissolved cavities (pH 2–3.5), **b** guard cell phytoliths with dissolved cavities (pH 2), **c** apparatus of stoma with dissolved cavities (pH 7), **d** dark, eroded *Picea*-blocky phytoliths (pH 2–10), **e** cracked or broken *Picea*-blocky phytoliths (pH 7-pH 12), **f** a cracked, eroded *Picea*-blocky phytolith and an epidermal phytolith with dissolved cavities (pH 10). Scale bar: 10 µm

and tissue phytoliths are distinguishable from each other after treatment at the same pH (these groups are marked in Fig. 9). The results of the PCA confirm that the most important elements causing dissimilarities among the studied phytoliths are carbon, calcium, potassium and sodium, as shown by loadings of the variables onto the first two principal components (Table 1). Relatively large negative values of carbon content have the effect that tissue phytoliths with higher carbon content are on the left side and ash

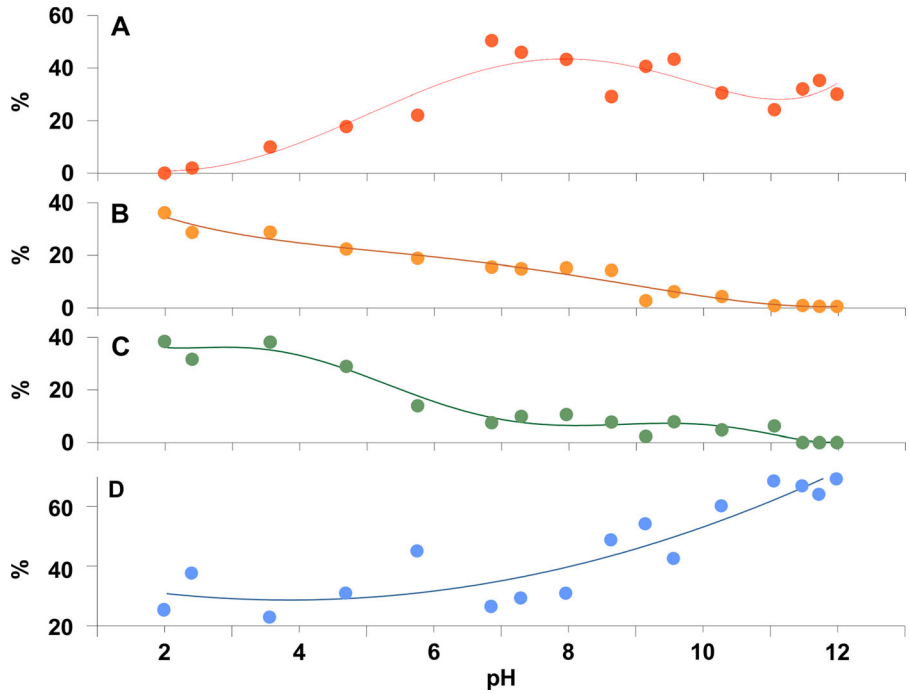

Fig. 5 Abundance of spruce needle (TN) phytolith types treated at different pH solutions. **a** eroded *Picea*-blocky phytoliths, **b** non-eroded *Picea*-blocky phytoliths, **c** tissue fragments, **d** other morphotypes

phytoliths with lower carbon content on the right side. Similarly, relatively high positive loadings of calcium and potassium show that ash phytoliths contain more of these elements than do tissue phytoliths, and their positions are located in opposite directions. Loading of sodium onto the second principal component results in a large positive value, illustrating that treated ash phytoliths, as well as tissue phytoliths, contained relatively large amounts of Na. At the same time, we could not find Na in the reference phytoliths or phytoliths in needles treated at pH 2.

Discussion

Solubility of phytoliths

Several studies have been done on the dissolution properties of silicon and phytoliths. Authors investigating this theme, however, used different extraction methods and different test subjects to describe silicon turnover, thus making it difficult to compare results between studies, and with our results (Cabanes et al. 2011; Cabanes and Shahack-Gross 2015; Haynes and Zhou 2018; Tran et al. 2018). Dissolution of "in situ" silicon, which is integrated into the tissues of needles, may be bound in several organic forms. Our results, therefore, would not be expected to be comparable with results of dissolution experiments on phytoliths released from plant tissues.

The pH-dependent dissolution of silica gel and diatomite in our experiment was similar to what has been reported in the literature (Morey et al. 1964; Krauskopf 1956; Tubana and Heckman 2015). We note that diatomite from Miocene sediments may be partially dissolved or leached.

Alkaline media (pH 8.0 or higher) increased the solubility of silicon in silica gel, diatomite and needle tissues and phytoliths. This finding has been recognized and used in plant nutrition in the last decade. For instance, Wang et al. (2018) established that 1% KOH-enhanced biochars, when added to soils, increase significantly the silicon available to plants.

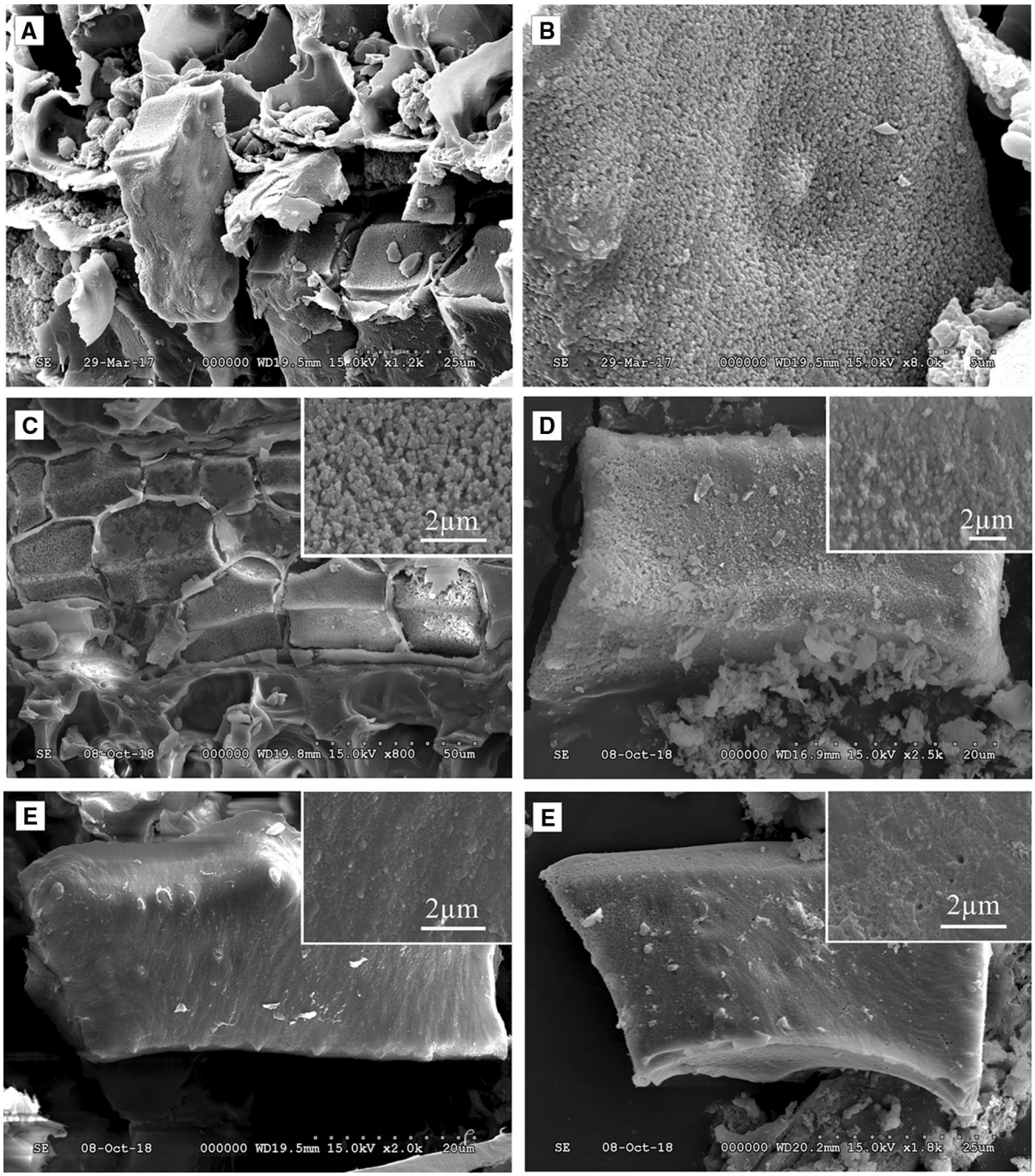

Fig. 6 SEM pictures of the spruce needle phytoliths (TN) treated at different pH solutions. The embedded photos highlight the surfaces of the phytoliths. **a** Control *Picea*-blocky phytoliths in the transfusion tissue of the needle, **b** tiny granules of control *Picea*-blocky phytolith, **c** phytoliths in the transfusion tissue at pH 2.0, **d** phytoliths in the TN ash at pH 2.0, **e** phytoliths in the transfusion tissue at pH 9.1, **f** phytoliths in TN ash at pH 9.1

Beyond the different Si dissolution curves at different pHs, the solubility of silicon from the needle tissues and from the phytoliths was much lower than from silica gel or diatomite. Specifically, the highest silicon solubility from needles was 13.6 mg L^{-1} at pH 8.0 and for the ash, 39.3 mg L^{-1} at pH 10.4. In

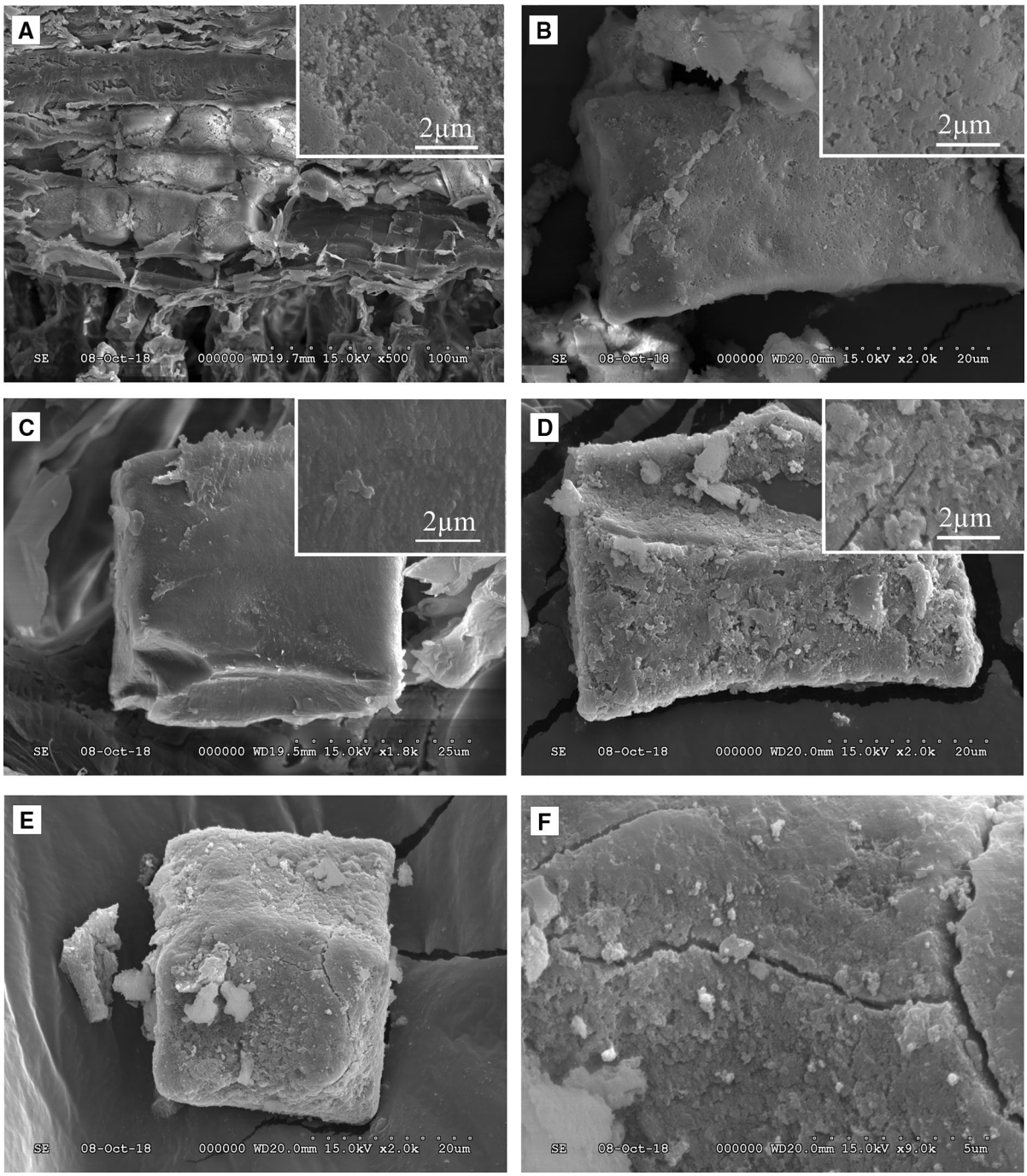

Fig. 7 SEM pictures of the spruce needle phytoliths (TN) treated at different pH solutions. The embedded photos highlight the surfaces of the phytoliths. **a** *Picea*-blocky phytoliths in the transfusion tissue at pH 10.4, **b** phytoliths in the TN ash at pH 10.4, **c** phytoliths in the transfusion tissue at pH 11.9, **d** phytoliths in the TN ash at pH 11.9, **e** phytoliths in the TN ash at pH 11.9, **f** surface of the phytoliths in TN ash at pH 11.9

contrast, from silica gel it was 217. 7 mg L^{-1} at pH 11.9 and from diatomite, was 216 mg L^{-1} at pH 11.9. The solubility of silicon from needles was about one-third the solubility from phytoliths, and we therefore concluded that the tissue of the needle protected the silicon from dissolution. A phytolith dissolution

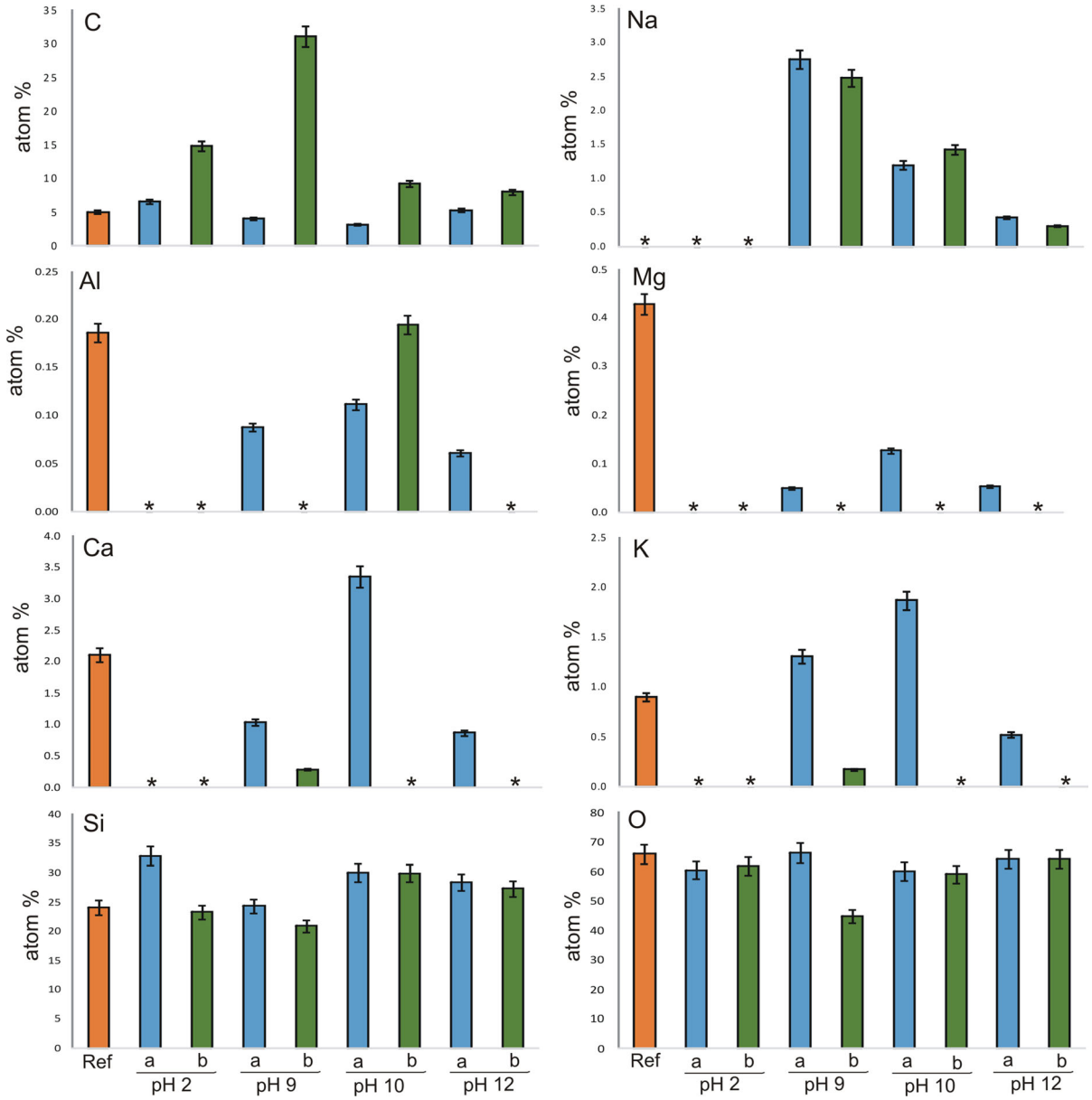

Fig. 8 Differences in element contents between phytoliths treated at acidic and alkaline pH. The diversity of elements in phytoliths was lower at acidic pH. Mean values ± 5% standard error of element content of the spruce needle phytoliths treated at different pH solutions. * = values below the threshold (0.1 atom%). Brown bars: element content of the reference phytoliths, blue bars: element content of the phytolith in TN ash, green bars: element content of the phytolith in the needle tissue. (Color figure online)

experiment was discussed by Cabanes and Shahack-Gross (2015), who compared the solubility of five modern and fossil phytolith assemblages at pH 10. This expanded on their earlier study (Cabanes et al. 2011), which showed that the solubility of modern plant phytolith assemblages was larger than values from fossils, and ranged between 3.3 and 4.1 mM Si (92.7–115.2 mg L^{-1}), and slightly greater than the solubility of silica gel at pH 10 (67.0 mg L^{-1}) in our experiment. Later authors found that the solubility of fossil phytoliths from sediments at two archaeological sites was less (1.6 to 2.1 mM Si [45.0–59.0 mg L^{-1}]), which probably resulted from the fossil phytoliths being more stable. Nevertheless, the solubility of these

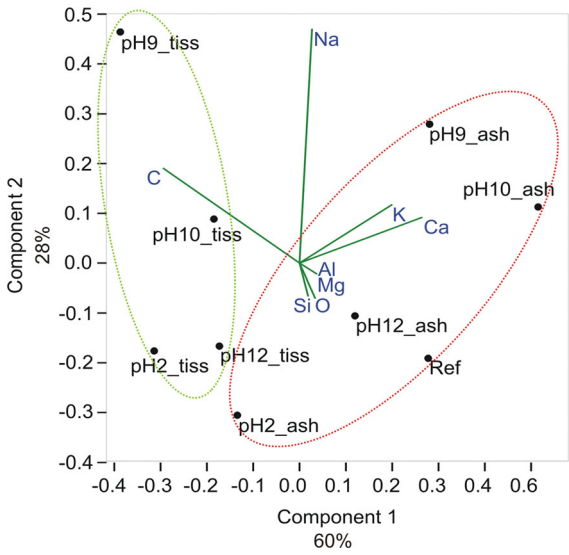

Fig. 9 Principal component analysis (PCA) score plot of the element content data of the phytoliths treated at different pH solutions

Table 1 Principal component analysis (PCA) on element content data was conducted to investigate which elements cause dissimilarities between the TN ash and the TA, as well as between the different pH treatments

	Axis 1 60%	Axis 2 28%	Axis 3 10%
C	**− 0.657**	0.355	0.593
O	0.076	− 0.132	− 0.112
Si	0.042	− 0.123	− 0.218
Ca	**0.590**	0.171	0.574
K	**0.446**	0.219	0.179
Na	0.060	**0.873**	− 0.436
Al	0.049	0.014	− 0.021
Mg	0.085	− 0.042	0.188

Loadings of each variable onto the first three principal components (PC). Variables with high loadings are shown in bold typeface

fossil phytoliths was ten times the solubility of silicon that originated from spruce needles in our study. Based on the Cabanes et al. (2012) measurements, as dissolution values > 3 mM Si [4.3 mg L^{-1}] indicate excellent preservation, values in our study were evidently low. Consequently, preservation of Si (and phytoliths) in needle tissue appears to be efficient. In addition, we note that biochemical processes in sediments may be more complicated. Nevertheless, Alfredsson et al. (2016) found that accelerated silicon dissolution processes by microbes in aquatic ecosystems cannot be assumed, as microbial activity does not increase Si release from phytoliths, in contrast to what occurs with diatoms. This finding suggests that silicon solubility from needle tissues is not accelerated measurably by microbial activity in natural sediments.

One result of our experiment, that Si solubility decreased between pH 8.0 and 11.1 in the needle tissues after day 2, suggests that needle tissue behaved similar to soil particles that adsorb silica maximally at pHs between these values (Haynes and Zhou 2018). SiO_2 monomers and oligomers precipitate on the surfaces of positive metal ions (Iller 1979). This pH range probably keeps silica in a more tightly bound condition, producing complexes in the tissues of the spruce needle, similar to what occurs in soils. The Si solubility from needles is highest between pH 6.9 and 9.1. This particular pH range is similar to the pH interval 6.8–9.6, typical of glacial lake and bog sediments (Ryan and Kahler 1987; Vocadlova et al. 2015). Solubility was most intense in this pH range, whereas phytoliths in the spruce needles were relatively well preserved after treatment.

Silica structures in plants are thought to represent the largest and most reactive silicon reservoir in soils, even compared with mineral quartz (Puppe et al. 2017), and in sediments (Tallberg et al. 2015). Natural abscission and accidental deforestation cause huge amounts of needle transport to glacial lakes. Ronchi et al. (2018) addressed the transfer of terrestrial siliceous material from the continent to the coast, but their findings may also hold for spruce forest/glacial lake systems, especially as stands of spruce forest in Norway show large Si uptake from soils (43 kg ha^{-1} - a^{-1}; Cornelis and Delvaux 2016). Ronchi et al. (2018) reported that up to 40 years after deforestation, peaks of Si content, a sign of Si export from deforested soils, are observed in rivers, and are attributed to erosion of the upper soil layer, which contains a large BSi pool. Our results thus remind researchers of the important role of spruce needles in the silicon biogeochemical cycle, and are useful in shedding light on the biogeochemical effects of deforestation and other land-use impacts.

The preservation of phytoliths in soils depends on soil depth and water availability (Alexandre et al. 1997; Derry et al. 2005; Blecker et al. 2006; Cabanes

and Shahack-Gross 2015). In that lake sediments, where the environment is considerably more humid, and pH can be predominantly alkaline (Ryan and Kahler 1987; Vocadlova et al. 2015), the chance of phytolith dissolution is higher. As our results show, dissolution may be moderated to some degree by needle tissues, including the thick epidermis and waxy cuticle. Phytoliths and silicon content were preserved three times more effectively in needle tissue than in ash. This durability may prove to be an advantage in paleoecological studies, in that fossil spruce needle silica and phytoliths may be useful tools, with respect to morphometrics, element composition and isotope ratios.

Changes of morphotypes

The two types of phytolith degradation seen in this study were observed earlier. Eroded forms of elongate psilate phytoliths, with heavily etched surfaces observed under a light microscope, were reported by Madella and Lancelotti (2012) and Strömberg et al. (2018). Tiny holes on the surfaces of the phytoliths, caused by dissolution, were reported by Osterrieth et al. (2009). These etched phytoliths, which originate from the needle epidermis cells and stomata, seem to be cell-wall silicified opals. Thus, this form of dissolution and erosion may reflect a distinctive characteristic of cell wall phytoliths (Hodson 2016; Alexandre et al. 2015).

The fact that a number of phytoliths in the 'other morphotype' group did not show considerable alteration as pH of the media increased, shows that the amount of dissolved Si in solution during the experiment originated in part from the diffuse silica pool of the apoplast of needle tissues. Moreover, it appears the Si was from partly dissolved surfaces of the phytoliths, not from the large number of totally dissolved phytoliths. The sign of partial dissolution was the dark (light microscopic), flat (SE microscopic) surface. Additionally, at alkaline pH, where dissolution was intense, less silicified tissue fragments were revealed. Consequently, at alkaline pH, disintegration of the tissues was more intense than at acidic pH.

The number of phytoliths was high in some cases, simply because of the number of broken pieces. Although the number of eroded *Picea*-blocky type phytoliths decreased between pH 8.0 and 11.1, as did the solubility of Si from needles, the number of the other morphotypes increased, and the number of tissue fragments decreased. These results demonstrate primarily that the Si solubility of the apoplast (cell walls and inter-cellular structures) was blocked at this pH range.

Dark (black or brown) phytoliths found in sediments and buried soils are interpreted as reflecting fire, and dark changed color is thought to reflect the burning of "occluded organic material" (Aleman et al. 2014). Dark fossil phytoliths, however, are also found in sediments of paleosols, where evidence of burning cannot be seen (Parr 2006). Boyd (2002) reported that plant samples contained dark carbon inclusions after being burned between 300 and 500 °C in a laboratory kiln. Some researchers observed naturally dark phytoliths in some Poaceae species. Other elements, in addition to carbon, can cause black or dark colors, and Wilding et al. (1967) found that the iron or manganese content of the soil correlated with the darkness of phytoliths. Our results show that in alkaline solution, some elements can be incorporated into the silica structure, and perhaps cause dark color.

We cannot dismiss the fact that a fossil phytolith may lose its fine, characteristic ornamentation after thousands of years. Experiments by Cabanes and Shahack-Gross (2015) and Osterrieth et al. (2009), however, showed that biogeochemical processes, which play a role in phytolith degradation, are not dependent primarily on the time scale.

Surface changes evaluated by SEM

Globular silica is typical for *Picea*-blocky phytoliths and is one of the known silica ultrastructure forms (Hodson 2016). The change in surface structure of spruce phytoliths caused by dissolution can also be brought about by natural processes in the environment. For example, Puppe and Leue (2018) studied Poaceae phytoliths by confocal laser scanning microscopy and reported that, compared to fresh phytoliths, the surface roughness of aged phytoliths decreased after deposition in soils. Correspondingly, Fraysse et al. (2009) described differences in specific surface areas of some phytoliths treated in mixed-flow reactors (25 °C, pH 1–9). Wilding and Drees (1974) also attributed the difference between solubility of phytoliths from trees and grasses to differences in specific surface areas, as was confirmed by Meunier et al. (2014). It seems that alteration of the globular ultrastructure and roughness

of the phytolith surface is a useful tool to estimate the degree of dissolution in the sediments.

Element content

At alkaline pH, the diversity of chemical elements in phytoliths was larger, as potassium, sodium, calcium, magnesium, and aluminum were found in the ash and tissue phytoliths. There was, however, no difference in carbon content of phytoliths at alkaline versus acid pH (measured by EDX). Therefore, it is unlikely that dark phytoliths obtain their color solely because of higher carbon content. Results of the PCA confirm that the most important elements that caused dissimilarities among the studied phytoliths were carbon, calcium, potassium and sodium. Between approximately pH 8.0 and 11.1, dissolution of silicon decreased, whereas element diversity increased at these pH values. Consequently, there may be a relationship between the element content and solubility of phytoliths, as suggested by the study of Osterrieth et al. (2009) in which elemental concentrations in eroded phytoliths were more diverse than in whole, intact ones.

The role of element content in phytolith solubility is not entirely clear (Puppe and Leue 2018). For example, aluminum content may affect solubility (Bartoli and Wilding 1980; Bartoli 1985), but at the same time, Fraysse et al. (2009) reported that aluminum had no effect on phytolith solubility. Additionally, phytoliths with different elemental contents would be sources for these elements, and phytolith dissolution could thus affect the biogeochemical cycles of these elements (Tran et al. 2018). As Osterrieth et al. (2009) suggested, the degradation process of phytoliths usually starts with the initial destruction of plant tissues. In some environments, extraneous elements may build up in the phytolith silica matrix when decomposition of the plant begins. Our experiment suggests that higher element content is an effect of the partial dissolution and is not the reason for more intense dissolution.

Conclusions

1. Dissolution of silicon in spruce needles was to some extent inhibited between pH 8.0 and 11.1. One reason may be that elements in needle tissues form complexes within and on the surfaces of silica. Needle tissue protects phytoliths against the erosion process at this alkaline pH range.
2. If, however, Si dissolution does occur, most dissolved silicon seems to originate from phytolith surfaces and the silica matrix of the apoplast in the tissues, rather than whole-phytolith dissolution. Evaluation of the number of phytoliths that underwent total dissolution is difficult.
3. Alkaline destruction and incorporation of extraneous elements caused the darkening of phytoliths. Our experiment suggests that extraneous metal elements are incorporated into the silica structure during the dissolution process. Higher element content is a consequence of partial dissolution, not the cause of dissolution.
4. The ultrastructure of the surface of the *Picea*-blocky type phytoliths, namely the disappearance of the globular structure, is a useful indicator of the degree of degradation in the sediments.
5. Our experimental treatments indicate that characteristic *Picea*-blocky phytoliths in Norway spruce needles may be well-preserved in some glacial lake sediments. Combined with other micro-analytical measurements, analyses of such phytoliths hold promise for paleoenvironmental reconstructions.

Acknowledgements Open access funding provided by MTA Institute for Nuclear Research (MTA ATOMKI). This research was supported by the European Union and the State of Hungary, co-financed by the European Regional Development Fund in project GINOP-2.3.2.-15-2016-00009 'ICER.' Author AP was supported by the János Bolyai Research Scholarship of the Hungarian Academy of Sciences; National Research, Development and Innovation Office (Grant Number PD_124607). The authors thank Krisztina Buczkó for providing the diatomite sample. We thank Timothy Jull for his comments on the manuscript and the editors and two anonymous reviewers for valuable suggestions that helped to improve the paper.

References

Albert RM, Weiner S (2001) Study of phytoliths in prehistoric ash layers using a quantitative approach. In: Meunier JD, Colin F (eds) Phytoliths—applications in earth science and human history. Balkema Publishers, Lisse, pp 251–266. https://doi.org/10.1201/noe9058093455.ch19

Aleman JC, Canal-Subitani S, Favier C, Bremond L (2014) Influence of the local environment on lacustrine sedimentary phytolith records. Palaeogeogr Palaeoclimatol Palaeoecol 414:273–283. https://doi.org/10.1016/j.palaeo.2014.08.030

Alexandre A, Meunier JD, Colin F, Koud JM (1997) Plant impact on the biogeochemical cycle of silicon and related weathering processes. Geochim Cosmochim Acta 61:677–682. https://doi.org/10.1016/S0016-7037(97)00001-X

Alexandre A, Basile-Doelsch I, Delhaye T, Borshneck D, Mazur JC, Reyerson P, Santos GM (2015) New highlights of phytolith structure and occluded carbon location: 3-D X-ray microscopy and NanoSIMS results. Biogeosciences 12:863–873. https://doi.org/10.5194/bg-12-863-2015

Alexandre A, Balesdent J, Cazevieille P, Chevassus-Rosset C, Signoret P, Mazur JC, Harutyunyan A, Doelsch E, Basile-Doelsch I, Miche H, Santos GM (2016) Direct uptake of organically derived carbon by grass roots and allocation in leaves and phytoliths: 13 C labeling evidence. Biogeosciences 13:693–1703. https://doi.org/10.5194/bg-13-1693-2016

Alfredsson H, Clymans W, Stadmark J, Conley DJ, Rousk J (2016) Bacterial and fungal colonization and decomposition of submerged plant litter: consequences for biogenic silica dissolution. FEMS Microbiol Ecol 92:fiw011. https://doi.org/10.1093/femsec/fiw011

Bartoli F (1985) Crystallochemistry and surface properties of biogenic opal. J Soil Sci 36:335–350. https://doi.org/10.1111/j.1365-2389.1985.tb00340.x

Bartoli F, Wilding LP (1980) Dissolution of biogenic opal as a function of its physical and chemical properties. Soil Sci Soc Am J 44:873–877. https://doi.org/10.2136/sssaj1980.03615995004400040043x

Blecker SW, McCulley RL, Chadwick OA, Kelly EF (2006) Biologic cycling of silica across a grassland bioclimosequence. Global Biogeochem Cycles 20:GB3023. https://doi.org/10.1029/2006gb002690

Boyd M (2002) Identification of anthropogenic burning in the paleoecological record of the northern prairies: a new approach. Ann Am Assoc Geogr 92:471–487. https://doi.org/10.1111/1467-8306.00300

Britton HTS, Robinson RA (1931) CXCVIII—universal buffer solutions and the dissociation constant of veronal. J Chem Soc Chem Soc. https://doi.org/10.1039/jr9310001456

Cabanes D, Shahack-Gross R (2015) Understanding fossil phytolith preservation: the role of partial dissolution in paleoecology and archaeology. PLoS ONE 10:e0125532. https://doi.org/10.1371/journal.pone.0125532

Cabanes D, Weiner S, Shahack-Gross R (2011) Stability of phytoliths in the archaeological record: a dissolution study of modern and fossil phytoliths. J Archaeol Sci 38:2480–2490. https://doi.org/10.1016/j.jas.2011.05.020

Cabanes D, Gadot Y, Cabanes M, Finkelstein I, Weiner S, Shahack-Gross R (2012) Human impact around settlement sites: a phytolith and mineralogical study for assessing site boundaries, phytolith preservation, and implications for spatial reconstructions using plant remains. J Archaeol Sci 39:2697–2705. https://doi.org/10.1016/j.jas.2012.04.008

Cornelis JT, Delvaux B (2016) The functional role of silicon in plant biology. Soil processes drive the biological silicon feedback loop. Funct Ecol 30:1298–1310. https://doi.org/10.1111/1365-2435.12704

Derry LA, Kurtz AC, Ziegler K, Chadwick OA (2005) Biological control of terrestrial silica cycling and export fluxes to watersheds. Nature 433:728–731. https://doi.org/10.1038/nature03299

Fraysse F, Pokrovsky OS, Schott J, Meunier JD (2009) Surface chemistry and reactivity of plant phytoliths in aqueous solutions. Chem Geol 258:97–206. https://doi.org/10.1016/j.chemgeo.2008.10.003

Hammer O, Harper DAT, Ryan PD (2001) PAST: paleontological statistics software package for education and data analysis. Palaeontologia Electronica 4:9

Hart TC (2016) Issues and directions in phytolith analysis. J Archaeol Sci 68:24–31. https://doi.org/10.1016/j.jas.2016.03.001

Haynes RJ, Zhou YF (2018) Effect of pH and added slag on the extractability of Si in two Si-deficient sugarcane soils. Chemosphere 193:431–437. https://doi.org/10.1016/j.chemosphere.2017.10.175

Hodson MJ (2016) The development of phytoliths in plants and its influence on their chemistry and isotopic composition. Implications for palaeoecology and archaeology. J Archaeol Sci 68:62–69. https://doi.org/10.1016/j.jas.2015.09.002

Hodson MJ, Sangster AG (1998) Mineral deposition in the needles of white spruce [*Picea glauca* (Moench.) Voss]. Ann Bot 82:375–385. https://doi.org/10.1006/anbo.1998.0694

Iller RK (1979) The chemistry of silica. Solubility, polymerization, colloid and surface properties, and biochemistry. Willey, Brisbane. https://doi.org/10.1002/ange.19800920433

Krauskopf KB (1956) Dissolution and precipitation of silica at low temperatures. Geochim Cosmochim Acta 10:1–46. https://doi.org/10.1016/0016-7037(56)90009-6

Latałowa M, van der Knaap WO (2006) Late quaternary expansion of Norway spruce *Picea abies* (L.) Karst. in Europe according to pollen data. Quat Sci Rev 25:2780–2805. https://doi.org/10.1016/j.quascirev.2006.06.007

Lisztes-Szabó Z, Braun M, Csík A, Pető Á (2019) Phytoliths of six woody species important in the Carpathians: characteristic phytoliths in Norway spruce needles. Veg Hist Archeobot 28:649–662. https://doi.org/10.1007/s00334-019-00720-x

Madella M, Lancelotti C (2012) Taphonomy and phytoliths: a user manual. Quat Int 275:76–83. https://doi.org/10.1016/j.quaint.2011.09.008

Magyari EK, Kunes P, Jakab G, Sümegi P, Pelánková B, Schabitz F, Braun M, Chytry M (2014) Late Pleniglacial vegetation in eastern-central Europe: are there modern analogues in Siberia? Quat Sci Rev 95:60–79. https://doi.org/10.1016/j.quascirev.2014.04.020

Mercader J, Astudillo F, Barkworth M, Bennett T, Esselmont C, Kinyanjui R, Grossman DL, Simpson S, Walde D (2010) Poaceae phytoliths from Niassa Rift, Mozambique. J Archaeol Sci 37:1953–1967. https://doi.org/10.1016/j.jas.2010.03.001

Meunier JD, Keller C, Guntzer F, Riotte J, Braun JJ, Anupama K (2014) Assessment of the 1% Na2CO3 technique to quantify the phytolith pool. Geoderma 216:30–35. https://doi.org/10.1016/j.geoderma.2013.10.014

Molnár A, Végvári Z (2017) Reconstruction of early holocene thermal maximum temperatures using present vertical distribution of conifers in the Pannon region (SE Central Europe). Holocene 27:236–245. https://doi.org/10.1177/0959683616658528

Mongay C, Cerda V (1974) A Britton–Robinson buffer of known ionic strength. Ann Chim 64:409–412. https://doi.org/10.1111/j.1749-6632.1974.tb53052.x

Morey GW, Fournier RO, Rowe JJ (1964) The solubility of amorphous silica at 25°C. J Geophys Res Biogeosci 69:10. https://doi.org/10.1029/jz069i010p01995

Nguyen NM, Dultz S, Guggenberger G (2014) Effects of pretreatment and solution chemistry on solubility of rice-straw phytoliths. J Plant Nutr Soil Sci 177:349–359. https://doi.org/10.1002/jpln.201300056

Osterrieth M, Madella M, Zurro D, Alvarez MF (2009) Taphonomical aspects of silica phytoliths in the loess sediments of the Argentinean Pampas. Quat Int 193:70–79. https://doi.org/10.1016/j.quaint.2007.09.002

Parr JF (2006) Effect of fire on phytolith coloration. Geoarchaeology 21:171–185. https://doi.org/10.1002/gea.20102

Piperno DR (2006) Phytoliths: a comprehensive guide for archaeologists and paleoecologists. AltaMira Press, Lanham. https://doi.org/10.1017/S0016756807003159

Puppe D, Leue M (2018) Physicochemical surface properties of different biogenic silicon structures: results from spectroscopic and microscopic analyses of protistic and phytogenic silica. Geoderma 330:212–220. https://doi.org/10.1016/j.geoderma.2018.06.001

Puppe D, Höhn A, Kaczorek D, Wanner M, Wehrhan M, Sommer M (2017) How big is the influence of biogenic silicon pools on short-term changes in water-soluble silicon in soils? Implications from a study of a 10-year-old soil–plant system. Biogeosciences 14:5239–5252. https://doi.org/10.5194/bg-14-5239-2017

Ran X, Liu J, Zang J, Xu B, Zhao S, Wu W, Wang H, Liu S (2018) Export and dissolution of biogenic silica in the Yellow River (Huanghe) and implications for the estuarine ecosystem. Mar Chem 200:14–21. https://doi.org/10.1016/j.marchem.2018.02.001

Ronchi B, Dassargues A, Batelaan O (2018) Dissolved Si export: impact of increased water fluxes through soil. Geoderma 312:151–158. https://doi.org/10.1016/j.geoderma.2017.10.011

Ryan DF, Kahler DM (1987) Geochemical and mineralogical indications of pH in lakes and soils in central New Hampshire in the early Holocene. Limnol Oceanogr 32:751–757. https://doi.org/10.4319/lo.1987.32.3.0751

Shillito LM (2011) Taphonomic observations of archaeological wheat phytoliths from neolithic Çatalhöyük, Turkey, and the use of conjoined phytolith size as an indicator of water availability. Archaeometry 53:631–664. https://doi.org/10.1111/j.1475-4754.2010.00582.x

Song Z, Wang H, Strong PJ, Shan S (2014) Increase of available soil silicon by Si-rich manure for sustainable rice production. Agron Sustain Dev 34:813–819. https://doi.org/10.1007/s13593-013-0202-5

Strömberg CAE, Dunn RE, Crifò C, Harris EB (2018) Phytoliths in paleoecology: analytical considerations, current use, and future directions. In: Croft D, Su D, Simpson S (eds) Methods in paleoecology: reconstructing cenozoic terrestrial environments and ecological communities, vertebrate paleobiology and paleoanthropology. Springer, Cham, pp 235–287. https://doi.org/10.1007/978-3-319-94265-0_12

Tallberg P, Opfergelt S, Cornelis JT, Liljendahl A, Weckström J (2015) High concentrations of amorphous, biogenic Si (BSi) in the sediment of a small high-latitude lake: implications for biogeochemical Si cycling and for the use of BSi as a paleoproxy. Aquat Sci 77:293–305. https://doi.org/10.1007/s00027-014-0387-y

Tran CT, Mai NT, Nguyen VT, Nguyen HX, Meharg A, Carey M, Dultz S, Marone F, Cichy SB, Nguyen MN (2018) Phytolith-associated potassium in fern: characterization, dissolution properties and implications for slash-and-burn agriculture. Soil Use Manag 34:28–36. https://doi.org/10.1111/sum.12409

Tubana BS, Heckman JR (2015) Silicon in soils and plants. In: Rodrigues FA, Datnoff LE (eds) Silicon and plant diseases. Springer, Cham, pp 7–51. https://doi.org/10.1007/978-3-319-22930-0_2

Vocadlova K, Petr L, Zackova P, Krizek M, Krizova L, Hutchinson SM, Sobr M (2015) The lateglacial and holocene in central europe: a multi-proxy environmental record from the bohemian forest, czech republic. Boreas 44:769–784. https://doi.org/10.1111/bor.12126

Wang H, Yoshiki S, Bi N, Sun X, Yang Z (2011) Recent changes of sediment flux to the western Pacific Ocean from major rivers in east and Southeast Asia. Earth Sci Rev 108:80–100. https://doi.org/10.1016/j.earscirev.2011.06.003

Wang M, Wang JJ, Wang X (2018) Effect of KOH-enhanced biochar on increasing soil plant-available silicon. Geoderma 321:22–31. https://doi.org/10.1016/j.geoderma.2018.02.001

Wilding LP, Drees LR (1974) Contributions of forest opal and associated crystalline phases to fine silt and clay fractions of soils. Clays Clay Miner 22:295–306. https://doi.org/10.1346/ccmn.1974.0220311

Wilding LP, Brown RE, Holowaychuk N (1967) Accessibility and properties of occluded carbon in biogenetic opal. Soil Sci 103:56–61. https://doi.org/10.1097/00010694-196701000-00009